Supplementary Information

Surface Microstructure Engenders Unusual Hydrophobicity in Phyllosilicates

Xinwen Ou,[a] Zhang Lin,[b] and Jingyuan Li*,[a]

[a]*Institute of Quantitative Biology and Department of Physics, Zhejiang University, Hangzhou 310027, China*
[b]*School of Environment and Energy, South China University of Technology, Guangzhou 510006, China*

Corresponding Author

*JY Li. Phone: +86 177 06437771; e-mail: jingyuanli@zju.edu.cn.

1. Crystal structures of substrate minerals.

Talc (triclinic, $C\bar{1}$ symmetry), having a chemical formula $Mg_3(Si_4O_{10})(OH)_2$, is a phyllosilicate mineral consists of silicate layers. One talc layer consists of two tetrahedral silicon sheets that are connected by one octahedral magnesium sheet, forming a TOT (tetrahedral-octahedral-tetrahedral) structure. The lattice constants of talc are determined by least squares refinement from X-ray diffraction photographs: a = 5.293 Å, b = 9.179 Å, c = 9.469 Å, α = 90.57°, β = 98.91°, γ = 90.03°.[1] The basal surface displays hexagonal Si-O rings formed by tetrahedral silicates, while OH group is located inside the hexagonal ring. Because the position of OH group is lower than the plane consisting of the hexagonal Si-O rings, there is periodic arrangement of hexagonal cavity on the surface. The talc substrate is terminated by the (001) plane, and the OH group in the bottom of the surface cavity orients perpendicular to the basal surface. A series of model systems are constructed by tuning the depth of surface cavity. More specifically, the OH group is moved to various positions and the depth of surface cavity, i.e. the vertical distance between the OH group and the plane of the hexagonal Si-O rings, ranges from 2.2 Å (natural talc) to 1.5, 1.0, 0.5 and 0 Å.

Mica (monoclinic, C2/c symmetry), with chemical formula $KAl_2(Si_3Al)O_{10}(OH)_2$, has also a TOT layer structure. And the depth of surface cavity is 2.2 Å, identical with talc. The lattice constants of mica are taken from high-resolution X-ray reflectivity: a = 5.1872 Å, b = 9.0070 Å, c = 20.0592 Å, $\alpha = \gamma = 90°$, $\beta = 95.804°$.[2] The basal surface of mica also contains hexagonal rings formed by tetrahedral silicates. While the OH group in the bottom of the surface cavity orients parallel to the basal surface. Besides, the chemical composition is somewhat different from talc counterpart due to partial substitution of Al (III) for Si (IV), resulting in a net negative structural charge which is neutralized by the naturally adsorbed potassium ions. The mica substrate is also cleaved by the (001) plane, and half the potassium ions remain for natural mica, i.e. 50% surface cavities are occupied by potassium ions. A series of model systems are constructed by adjusting the surface coverage of potassium ions from 50% (natural mica) to 37.5%, 25%, 12.5% and 0%. As the impact of internal atomic charge on the interfacial property should be minor,[3] the partial charge of inner potassium ions between the silicate layers is modified accordingly to maintain overall charge neutrality.

2. Methods for simulation details.

The CLAYFF force field is used to describe the interaction of minerals.[4] For water molecules, the extended simple point charge (SPC/E) potential is chosen.[5] The particle-mesh Ewald method with a real space cutoff of 10 Å is used to compute electrostatic interactions,[6] whereas a 10 Å cutoff is applied to van der Waals interactions. An aqueous region with the thickness of 90 Å is placed above the constructed substrate. Each system is relaxed by a standard equilibration procedure, including a standard conjugate gradient minimization and 2000 ps *NVT* (300 K) simulation. The equilibrated systems then undergo 8000 ps production run in *NVT* ensemble at 300 K, and the equilibrium trajectory for each system is recorded for statistical analysis at 1 ps intervals. All simulations are performed with Gromacs 4.6.5 package.[7]

3. Computational details about the number of hydrogen bonds and surface density distributions.

A geometric definition of the hydrogen bond (HB) is adopted from previous works, namely, two water molecules are considered to be hydrogen bonded if the oxygen-oxygen distance is less than 3.5 Å, and the angle of O-H…O is less than 30° simultaneously.[8] The HB number profile is obtained by statistically summing up the HB number associated with water molecules positioned at a certain distance of water oxygen atom from the surfaces and then dividing it by the number of those water molecules. The calculation process is similar to the previous studies.[9]

The x-y surface density distributions of interfacial water are measured by calculating the average number of water oxygen atoms in the first hydration layer. More specifically, the talc (001) surface is divided into the square cells with the size of 0.1 Å, and the water molecules within the first hydration layer are considered (e.g. $z < 3.6$ Å for natural talc). For each cell, the time-averaged number of water oxygen atoms is calculated separately and then normalized by the maximum number of water oxygen atoms in the cell. The calculation process is similar to the previous studies.[10]

4. Methods to compute the contact angles.

The contact angle of a water droplet on the surface is measured following a similar procedure of our previous study.[11] We first prepare a water droplet of ~1000 water molecules with an initial rectangular shape, and the droplet is then placed on the surface of substrate within a periodic simulation box whose size is sufficiently large to reduce the periodic image effect of water droplet. The system is equilibrated for 1000 ps, and then a 2000 ps production data (*NVT* ensemble at 300 K) is collected for analysis. The contact angle is determined by fitting the liquid/vapor interface to a circle (see Fig. S1) by averaging 2000 frames. Here, the liquid/vapor interface is defined as where the water number density falls to less than one-half that of the bulk. More specifically, the droplet is divided into thin slices with a width of 1 Å parallel to the basal plane of the substrate, and water number density in each bin is calculated separately.

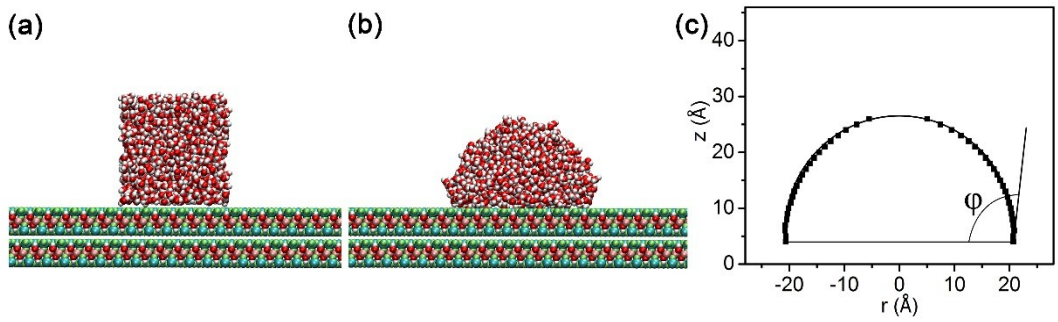

Fig. S1 (a) The starting configuration (i.e. t = 0 ps) for the water contact angle simulation on talc (001) surface; (b) representative snapshot after equilibration; (c) profile of the water/vapor interface, fitted with a circle for the contact angle calculation.

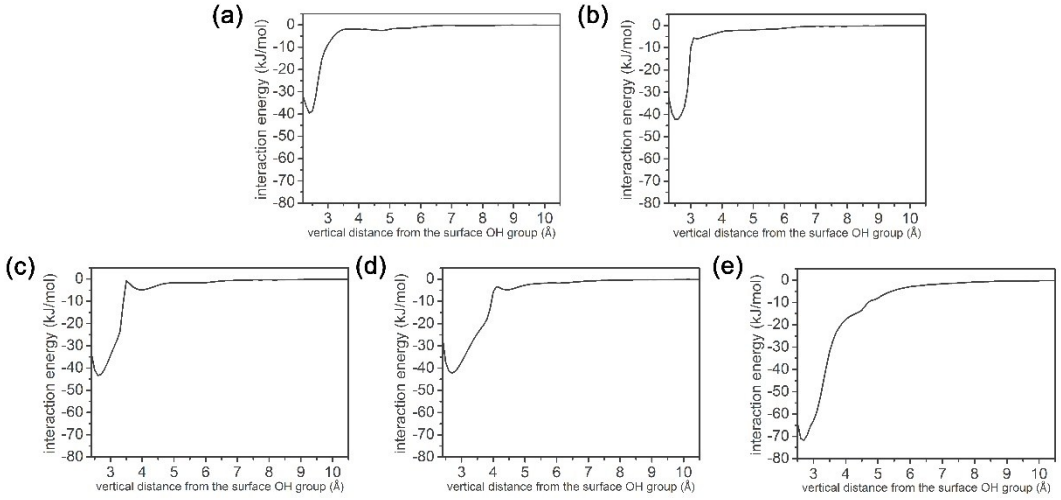

Fig. S2 The interaction energy between water molecule and talc substrate with different cavity depth: h = 0 Å (a), h = 0.5 Å (b), h = 1.0 Å (c), h = 1.5 Å (d), and h = 2.2 Å (e).

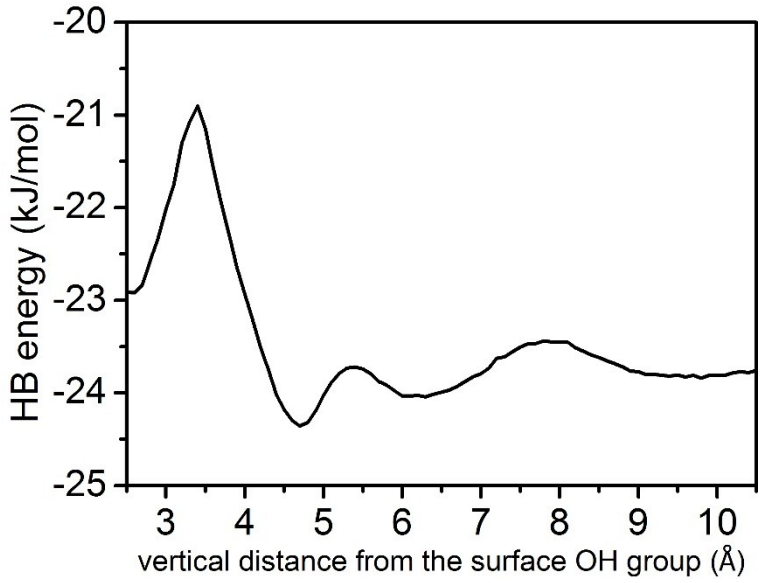

Fig. S3 The averaged hydrogen bond energy in water-water interaction for natural talc, i.e. h = 2.2 Å. The hydrogen bond energy is defined as the interaction energy between a water pair connected by a hydrogen bond.

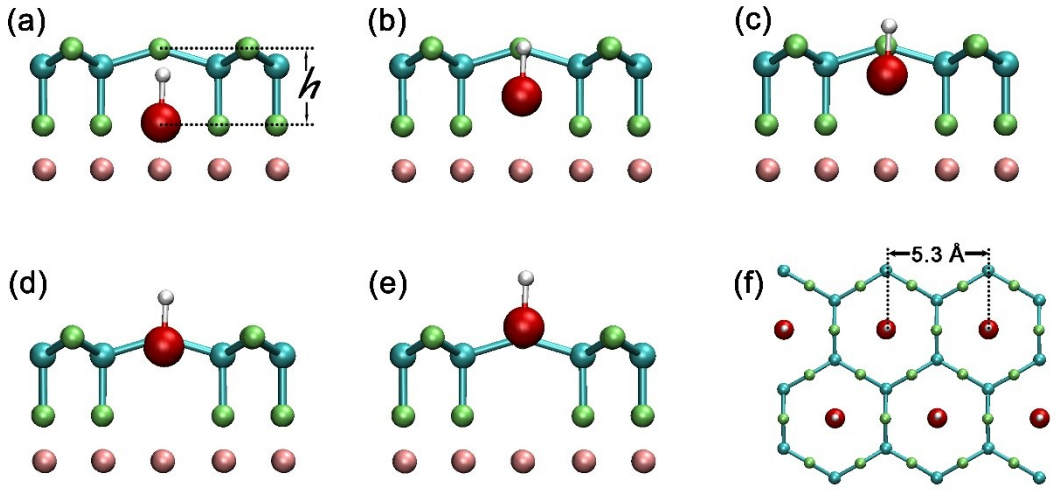

Fig. S4 The side view of surface cavity of talc with different cavity depth: h = 2.2 Å (a), h = 1.5 Å (b), h = 1.0 Å (c), h = 0.5 Å (d), h = 0.0 Å (e); and top view of talc (f). The definition of the depth of surface cavity, h, and the separation between adjacent cavities are also illustrated in the snapshots.

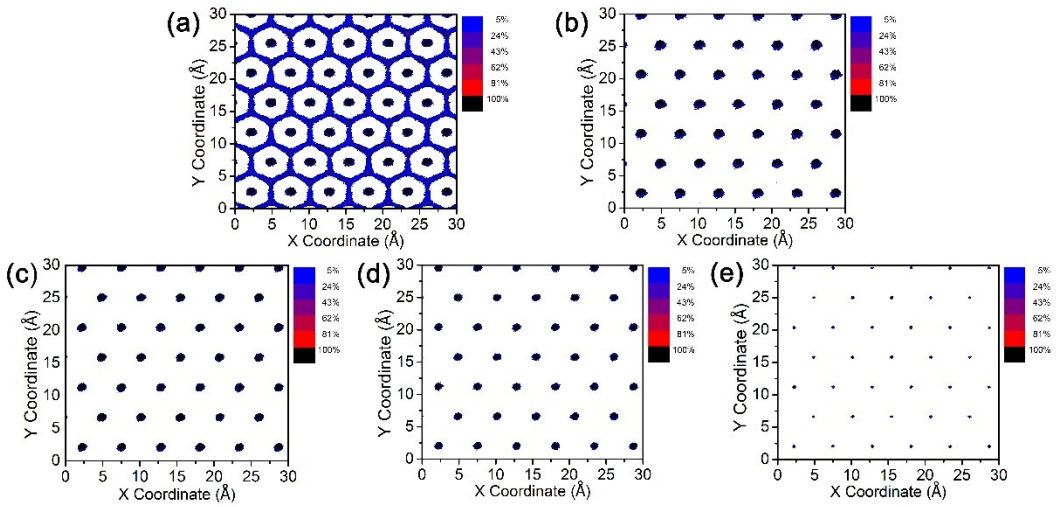

Fig. S5 Surface density distribution of water oxygen in the first hydration layer for talc systems different cavity depth: h = 0 Å (a), h = 0.5 Å (b), h = 1.0 Å (c), h = 1.5 Å (d), and h = 2.2 Å (e). The color scale illustrates the normalized probability distributions (in arbitrary units) of the water oxygen.

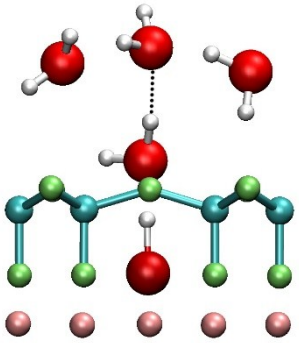

Fig. S6 The snapshot illustrates the interaction of the trapped water with the other water molecules. The trapped water molecule can only form one hydrogen bond with the water molecule right on its top.

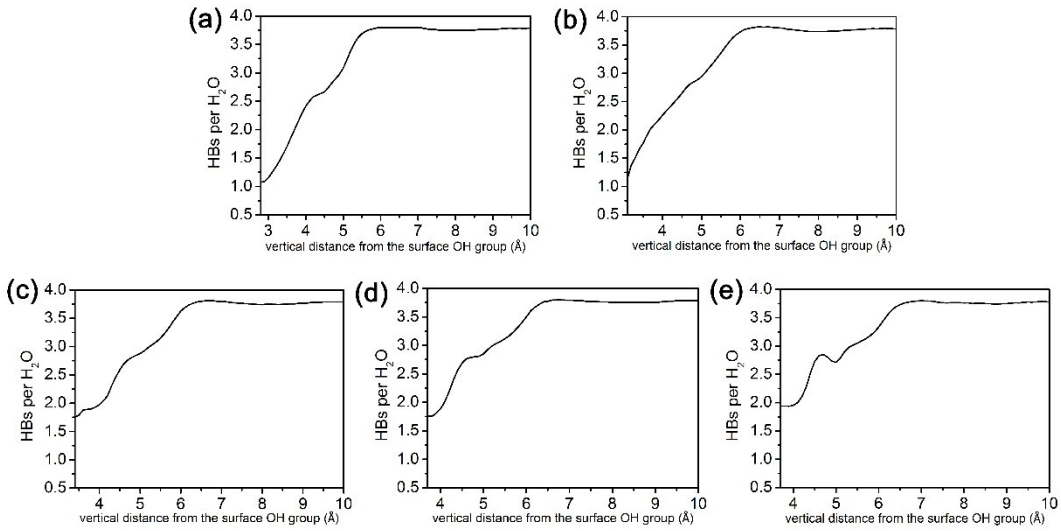

Fig. S7 The average number of hydrogen bonds per water molecule on mica (001) surface with different surface coverage of potassium ions: 0% (a), 12.5% (b), 25% (c), 37.5% (d) and 50% (e).

References

1 J. H. Rayner and G. Brown, *Clays Clay Miner.*, 1973, **21**, 103-114.

2 M. L. Schlegel, K. L. Nagy, P. Fenter, L. Cheng, N. C. Sturchio and S. D. Jacobsen, *Geochim. Cosmochim. Acta*, 2006, **70**, 3549-3565.

3 N. Giovambattista, P. J. Rossky and P. G. Debenedetti, *Phys. Rev. E*, 2006, **73**, 041604.

4 R. T. Cygan, J.-J. Liang and A. G. Kalinichev, *J. Phys. Chem. B*, 2004, **108**, 1255-1266.

5 H. J. C. Berendsen, J. R. Grigera and T. P. Straatsma, *J. Phys. Chem.*, 1987, **91**, 6269-6271.

6 U. Essmann, L. Perera, M. L. Berkowitz, T. Darden, H. Lee and L. G. Pedersen, *J. Chem. Phys.*, 1995, **103**, 8577-8593.

7 B. Hess, C. Kutzner, D. van der Spoel and E. Lindahl, *J. Chem. Theory Comput.*, 2008, **4**, 435-447.

8 H. F. Xu and B. J. Berne, *J. Phys. Chem. B*, 2001, **105**, 11929-11932.

9 (a) X.-P. Ren, B. Zhou, L.-T. Li and C.-L. Wang, *Chin. Phys. B*, 2013, **22**, 016801; (b) U. Terranova and N. H. de Leeuw, *J. Chem. Phys.*, 2016, **144**, 094706; (c) D. Argyris, D. R. Cole and A. Striolo, *J. Phys. Chem. C*, 2009, **113**, 19591-19600; (d) D. Argyris, T. Ho, D. R. Cole and A. Striolo, *J. Phys. Chem. C*, 2011, **115**, 2038-2046; (e) H. Du and J. D. Miller, *J. Phys. Chem. C*, 2007, **111**, 10013-10022; (f) X. Ou, J. Li and Z. Lin, *J. Phys. Chem. C*, 2014, **118**, 29887-29895; (g) O. Z. Tan, K. H. Tsai, M. C. H. Wu and J.-L. Kuo, *J. Phys. Chem. C*, 2011, **115**, 22444-22450.

10 (a) N. Giovambattista, P. J. Rossky and P. G. Debenedetti, *J. Phys. Chem. B*, 2009, **113**, 13723-13734; (b) D. Argyris, N. R. Tummala, A. Striolo and D. R. Cole, *J. Phys. Chem. C*, 2008, **112**, 13587-13599; (c) N. Giovambattista, P. G. Debenedetti and P. J. Rossky, *J. Phys. Chem. C*, 2006, **111**, 1323-1332; (d) Y. Qiu, Y. Liu, Y. Tu, C. Wang and Y. Xu, *J. Phys. Chem. C*, 2017, **121**, 17365-17370; (e) M. C. F. Wander and A. E. Clark, *J. Phys. Chem. C*, 2008, **112**, 19986-19994; (f) D. Argyris, D. R. Cole and A. Striolo, *Langmuir*, 2009, **25**, 8025-8035; (g) T. A. Ho, D. V. Papavassiliou, L. L. Lee and A. Striolo, *Proc Natl*

Acad Sci U S A, 2011, **108**, 16170-16175.
11 X. Li, J. Li, M. Eleftheriou and R. Zhou, *J. Am. Chem. Soc.*, 2006, **128**, 12439-12447.